International Journal of Pharmaceutics 427 (2012) 185–191

Contents lists available at SciVerse ScienceDirect

International Journal of Pharmaceutics

journal homepage: www.elsevier.com/locate/ijpharm

Constant size, variable density aerosol particles by ultrasonic spray freeze drying

Suzanne M. D'Addio[a,b], John Gar Yan Chan[a], Philip Chi Lip Kwok[a], Robert K. Prud'homme[b], Hak-Kim Chan[a,*]

[a] Advanced Drug Delivery Group, Faculty of Pharmacy, The University of Sydney, Camperdown, NSW 2006, Australia
[b] Chemical and Biological Engineering, Princeton University, Princeton, NJ 08854, USA

ARTICLE INFO

Article history:
Received 24 November 2011
Received in revised form 19 January 2012
Accepted 24 January 2012
Available online 1 February 2012

Keywords:
Inhalation aerosol
Porous particles
Fine Particle Fraction
Spray freeze
Ultrasonic atomization

ABSTRACT

This work provides a new understanding of critical process parameters involved in the production of inhalation aerosol particles by ultrasonic spray freeze drying to enable precise control over particle size and aerodynamic properties. A series of highly porous mannitol, lysozyme, and bovine serum albumin (BSA) particles were produced, varying only the solute concentration in the liquid feed, c_s, from 1 to 5 wt%. The particle sizes of mannitol, BSA, and lysozyme powders were independent of solute concentration, and depend only on the drop size produced by atomization. Both mannitol and lysozyme formulations showed a linear relationship between the computed Fine Particle Fraction (FPF) and the square root of c_s, which is proportional to the particle density, ρ, given a constant particle size d_g. The FPF decreased with increasing c_s from 57.0% to 16.6% for mannitol and 44.5% to 17.2% for lysozyme. Due to cohesion, the BSA powder FPF measured by cascade impaction was less than 10% and independent of c_s. Ultrasonic spray freeze drying enables separate control over particle size, d_g, and aerodynamic size, d_a which has allowed us to make the first experimental demonstration of the widely accepted rule $d_a = d_g(\rho/\rho_o)^{1/2}$ with particles of constant d_g, but variable density, ρ (ρ_o is unit density).

1. Introduction

Pulmonary drug delivery by aerosol inhalation has been rapidly emerging over the past two decades for pharmacologic treatments of asthma, chronic obstructive pulmonary disease, respiratory infection (Weers et al., 2010) and pulmonary arterial hypertension (Olschewski et al., 2002). To be effective for pulmonary drug delivery, aerosol particles must deposit at the appropriate sites in the lungs. Aerodynamic diameter, d_a, is the key determinant for deposition in the respiratory tract (Borgstrom and Clark, 2002). For spherical particles, d_a is governed by both the particles' geometric diameter (d_g) and density (ρ) (Hinds, 1999):

$$d_a = d_g\left(\frac{\rho}{\rho_o}\right)^{1/2} \quad (1)$$

where ρ_o is unit density (i.e. 1 g cm^{-3}). Hence, a small aerodynamic diameter can be achieved for large particles with a low density. Indeed, porous particles with a low density (<0.4 g cm^{-3}) have been explored for enhanced aerosol performance of both small and large molecular drugs for pulmonary delivery (Amorij et al., 2007; Chew and Chan, 2001; Edwards et al., 1997; Maa et al., 1999; Mohri et al., 2010; Saluja et al., 2010; Sweeney et al., 2005; Zijlstra et al., 2007).

One method of producing large porous particles is spray freeze drying (SFD). The steps involved in producing particles in this process are: atomization, rapid freezing, and lyophilization. Atomization using an ultrasonic nozzle has the distinct advantages of (i) a narrow droplet size distribution that can be controlled (Topp and Eisenklam, 1972) and (ii) no additional air flow, so drops are efficiently captured in a liquid cryogen. Due to phase separation of solids from the ice crystals during freezing, the removal of ice by lyophilization results in voids in the final dried particles (Qian and Zhang, 2011). The overall particle size is determined by the size of the frozen droplet, while the aerodynamic diameter of the particle is governed by the particle size and the voids according to Eq. (1).

Maa et al. (1999) pioneered the development of spray freeze drying for the production of pharmaceutical powders, but concluded that only with two-fluid nozzle atomization at high air flow rates could aerosol particles with FPF >30% be produced and that the large, porous particles produced specifically with ultrasonic atomization had poor aerodynamic performance. Subsequent studies investigated spray freeze drying with ultrasonic atomization for protein encapsulation. The powders were evaluated for nasal delivery (Garmise et al., 2007), epidermal powder immunization

Abbreviations: d_a, aerodynamic diameter; d_g, geometric diameter; ρ, density; d_{mode}, diameter corresponding to the mode of the particle size distribution; BSA, bovine serum albumin; DPI, dry powder inhaler; FPF, Fine Particle Fraction; LN_2, liquid nitrogen; NGI, Next Generation Impactor; PSD, particle size distribution; SFD, spray freeze dry.

* Corresponding author at: Pharmacy Building A15, University of Sydney, NSW 2006, Australia. Tel.: +61 2 9351 3054; fax: +61 2 9351 6950.
E-mail address: kim.chan@sydney.edu.au (H.-K. Chan).

0378-5173/$ – see front matter © 2012 Elsevier B.V. All rights reserved.
doi:10.1016/j.ijpharm.2012.01.048

(Maa et al., 2003, 2004), or injection (Nguyen et al., 2004) and so aerodynamic properties were not examined. A study by Costantino et al. (2000) used a two-fluid nozzle atomizer for the production of aerosolizable dry powders, highlighting the effects of atomization conditions on the resulting particle size and protein stability, without systematically varying protein concentration. Previously, it had been appreciated that the size of particles produced by spray freeze drying is dominated by the aqueous droplet size at both low (Bi et al., 2008) and high (Maa et al., 2004) concentrations. However, the influence of the solute concentration in the atomized solution on aerosol performance of the resulting dry particles has not been quantitatively explored in prior studies, nor used to optimize delivery to the lungs.

Recently, we investigated aerosol drug delivery of functional nanocarriers embedded in micron-sized matrix particles (D'Addio et al., 2011). During the course of our study, we prepared and characterized mannitol, lysozyme, and bovine serum albumin particles prepared by spray freeze drying. Based on the aerodynamic properties of powders produced, we found that the combination of an ultrasonic atomization nozzle with spray freeze drying enabled unique and unexpected control over the aerosol properties of dry powders through the concentration of the feed solution. This specific combination of processing techniques enables control over particle properties which has not been previously achieved. The results establish a functional relationship between FPF and formulation concentration that supports the theoretically relationship between aerodynamic diameter and particle density (i.e. Eq. (1)).

2. Experimental

2.1. Spray freeze drying

To form microparticles, solutions of mannitol (Pearlitol 160C, Roquette, Lestrem, France), bovine serum albumin (BSA, Sigma–Aldrich, St. Louis, MO, USA), or lysozyme (Sigma–Aldrich, St. Louis, MO, USA) at concentrations (c_s) of 10, 20, 40 or 50 mg cm^{-3} in deionized water were fed via a digitally controlled syringe pump (Model PHD 2000, Harvard Apparatus, Holliston, MA) at 0.5 mL min^{-1} into a CV-24 ultrasonic nozzle powered by a Vibra Cell 40 kHz ultrasonic generator (Sono-Tek Corp., Milton, NY). The atomized droplets fell 3–10 cm, via gravity, and were collected in liquid nitrogen (LN_2). The nozzle height had no effect on drop size, but had to be far enough above the liquid nitrogen to avoid freezing the solution in the atomizer. After spraying of the solution was complete, the excess LN_2 was allowed to boil off and the frozen droplets were lyophilized in a Christ Alpha 1-4 LOC-1M freeze dryer (Martin Christ, Osterode am Harz, Germany). Mannitol was freeze dried at 25 °C for 18 h, whereas BSA and lysozyme were first maintained at −25 °C for 48 h and then at 20 °C for 24 h.

2.2. Particle sizing by laser diffraction

Volume weighted particle size distributions of the powders were measured after freeze drying. The samples were dispersed in a 1 bar stream of air by a Scirocco 2000 dry powder feeder (Malvern, Worcestershire, UK) and then sized by a Masterizer 2000 (Malvern, Worcestershire, UK) using laser diffraction with an obscuration between 0.3% and 10%. The particle refractive indices were 1.544 for mannitol and 1.445 for BSA and lysozyme. The absorption for all three compounds was 0.1. The dispersant refractive index was 1.000 for air. The diameters corresponding to the cumulative volume under 10, 50 and 90% were reported as the d_{10}, d_{50} and d_{90}, respectively. The span was then computed as $(d_{90} - d_{10})/d_{50}$. The size of deionized water droplets produced by the ultrasonic nozzle was determined using a Spraytec spray particle analyzer (Malvern, Worcestershire, UK) over 10 s of continuous spraying with 1 s data collection time. The nozzle was situated at about 3 cm above the laser to mimic the distance above the liquid nitrogen surface in SFD. The real and imaginary refractive indices for deionized water were 1.33 and 0.00, respectively. All measurements were performed in triplicate.

2.3. Particle imaging

Images of spray freeze dried powders were obtained using a field emission scanning electron microscope (SEM) (Zeiss Ultra Plus, Carl Zeiss NTS GmbH, Oberkochen, Germany) at 2 kV. The samples were prepared on carbon tape and sputter coated with approximately 11.3 nm palladium/gold using a K550X sputter coater (Quorum Emitech, Kent, UK) before imaging.

2.4. Differential scanning calorimetry (DSC)

The thermal properties of each of the spray-dried mannitol powders were analyzed using a differential scanning calorimeter (DSC, Model 821e, Mettler Toledo. Greifensee, Switzerland). Samples (3–5 mg) were crimp-sealed in 40 μL aluminum crucibles with a vent hole in the lid and heated from 30 to 180 °C at a heating rate of 10 °C min^{-1} under 250 cm^3 min^{-1} nitrogen purge.

2.5. X-ray diffraction (XRD)

Diffraction patterns for spray freeze dried powders were characterized using X-ray powder diffraction (D5000, Siemans, Munich, Germany). Samples for XRD were spread on glass slides and subjected to Cu Kα radiation at 30 mA and 40 kV. The scattered intensity was collected by a detector at 5–40° 2θ, at a step rate of 0.04° 2θ s^{-1}.

2.6. Particle dispersion

The dispersion properties of the powders were determined using a Next Generation Impactor (NGI) (Copley Scientific, Nottingham, UK). Particles dispersed in an air stream were conveyed through the instrument and impacted on the eight consecutive stages based on the well-characterized aerodynamic size cut-offs. Before each run, all stages were coated with a fine silicone spray (Slipicone, DC Products, Waverly, VIC, Australia) to minimize bouncing. The flow rate through the NGI was set to 100 L min^{-1} using a rotary vane vacuum pump (Model RA 0025 F 505, Busch, Maulburg, Germany) and calibrated flow meter (TSI 3063, TSI Instruments Ltd., Buckinghamshire, UK). At this condition, the aerodynamic diameter cut-off for particles captured on stages S1, S2, S3, S4, S5, S6 and S7 are 6.1, 3.4, 2.2, 1.3, 0.7, 0.4 and 0.2 μm, respectively. A filled capsule, containing 2.5–5 mg of powder, was placed into the sample compartment of an Aerolizer® DPI, the inhaler was activated, inserted into a United States Pharmacopoeia (USP) throat, and tested for 2.5 s at 100 L min^{-1}. After the run, the inhaler, capsule, throat, and all sample stages were washed with 4 mL of water which was assayed for solute concentration by HPLC as described below. Each powder was tested in triplicate.

2.7. High performance liquid chromatography

Quantification of mannitol deposition was performed using high performance liquid chromatography (HPLC) on the 4 mL of water used to wash each stage (Model LC-20, Shimadzu, Kyoto, Japan). For the assay, a refractive index detector (Model RID-10A, Shimadzu, Kyoto, Japan) was used. Samples were injected (100 μL) into a Resolve C-18 column, 5 μm, 150 mm × 3.9 mm (Waters, Milford, MA) with de-ionized and filtered water as mobile phase, at a

flow rate of 1 mL min^{-1}. A calibration curve was constructed using standard solutions from 1 to 1000 μg mL^{-1}.

BSA samples were injected into a BioSep-SEC-S 300 column, 300 mm × 7.8 mm (Phenomenex, Sydney, NSW, Australia) with a 0.05 M potassium dihydrogen orthophosphate mobile phase (adjusted to pH 7.4 with NaOH) at a flow rate of 1 mL min^{-1}. The detection wavelength was 214 nm and the concentration of BSA was calculated with reference to the standard curve.

2.8. UV-Vis spectrophotometry

Lysozyme concentrations were determined by measuring UV absorbance of the solutions using a Hitachi U-2000 UV spectrophotometer (Hitachi, Tokyo, Japan) at a wavelength of 280 nm. A standard curve was constructed for lysozyme solutions from 3.8×10^{-3} to 3.8×10^{-1} mg mL^{-1}.

3. Results

3.1. Particle sizing by laser diffraction

The particle size distributions (PSD) of the spray freeze dried (SFD) powders measured by laser diffraction for all formulations are plotted in Fig. 1. The 40 kHz ultrasonic frequency used to atomize aqueous solutions produced dry particles with size distributions that had similar main peak locations. A SFD formulation of mannitol was dispersed in an air stream at dispersing pressure increasing from 0.5 bar to 3.5 bar. It was found that the d_{50} value and span measured at each condition decreased and increased, respectively, with dispersion pressure (Fig. 2). A similar trend was observed for lysozyme particles. Since the mode of each distribution, d_{mode}, corresponded to the population of primary particles, this was used to compare the primary particle size for each formulation. Across the twelve formulations, the d_{mode} fell within a relatively narrow range from, 17.2 to 37 μm (Table 1). The d_{mode} values are equivalent for particles produced from the same material, independent of the aqueous solution concentration. In general, the span values were small, especially for lysozyme particles. The span was computed as a measure of the breadth of the distribution, and was accordingly larger in cases where there were satellite peaks or shoulders on the main peak for mannitol and BSA in the PSD. The deionized water droplets produced by the ultrasonic nozzle were found to have a d_{mode} = 48.3 μm and had a narrow, monomodal distribution of sizes (Fig. 3), corresponding to a span of 0.9. All of the particle size measurements were performed using instruments which use Mie scattering theory.

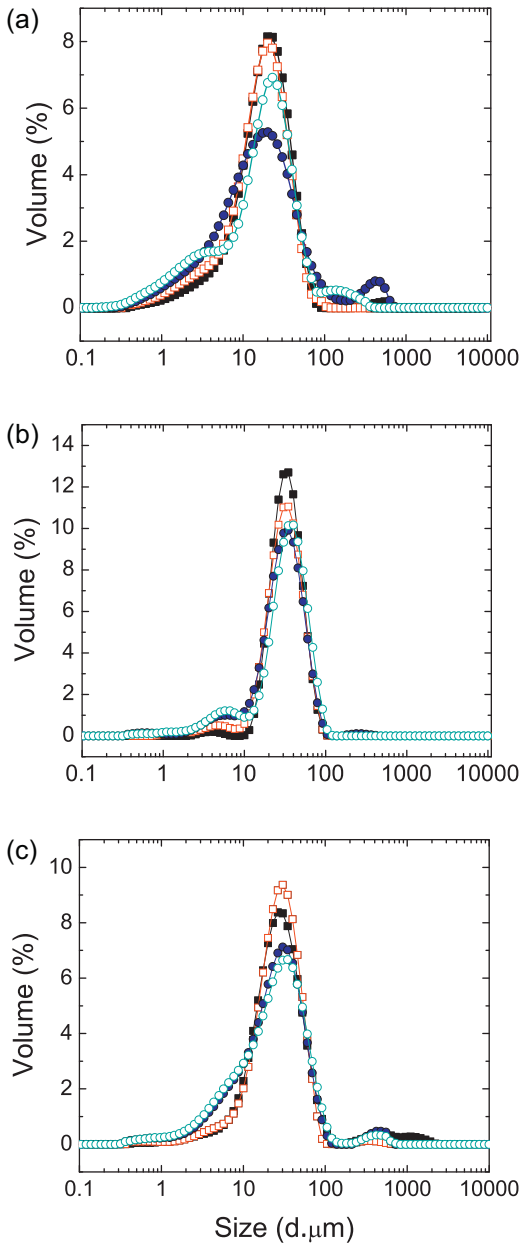

Fig. 1. Volume weighted size distributions for each particle formulation, where each was prepared from a solution of (a) mannitol, (b) lysozyme, or (c) BSA in water at a concentration of 1 wt% (■), 2 wt% (□), 4 wt% (●), and 5 wt% (○).

3.2. SEM imaging

Representative secondary electron micrographs of spray freeze dried mannitol, BSA and lysozyme particles are shown in Fig. 4. The images support the use of d_{mode} as an approximation of the primary dried particle size. The particles all appeared spherical and porous, which were morphologies that have previously been observed for spray freeze dried particles prepared in this concentration range (Costantino et al., 2000; Lee et al., 2002). Qualitatively, the spherical shape of the particles became better defined as the feed solution concentration (c_s) was increased (left to right in Fig. 4). Furthermore, there is less apparent void space in similarly sized particles, corresponding to their increased density.

Table 1
The mode and span of each particle size distribution in Fig. 1.

Formulation	Mannitol		Lysozyme		BSA	
c_s (mg cm^{-3})	d_{mode} (μm)	Span	d_{mode} (μm)	Span	d_{mode} (μm)	Span
10	19.6 ± 5.6	1.9 ± 0.1	33.2 ± 2.6	1.1 ± .02	28.9 ± 2.2	2.0 ± 0.3
20	20.0 ± 5.3	1.9 ± 0.2	33.2 ± 2.6	1.3 ± .08	30.2 ± 0.0	1.6 ± .02
40	17.2 ± 3.6	4.2 ± 1.7	34.8 ± 0.0	1.6 ± .03	30.2 ± 0.0	2.2 ± .01
50	20.9 ± 4.1	2.8 ± 1.1	37.3 ± 3.6	1.6 ± 0.1	31.7 ± 2.6	2.4 ± 0.1

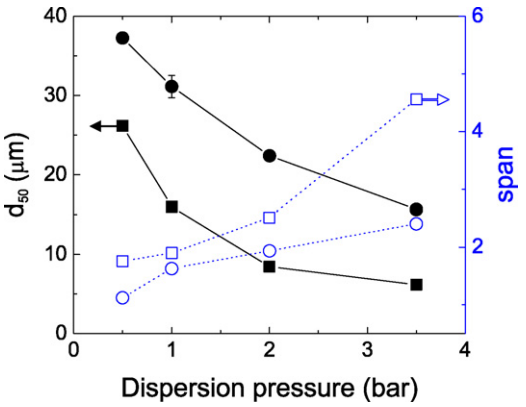

Fig. 2. The d_{50} of the measured PSD for SFD mannitol (■) and lysozyme (●) particles, determined at various dispersion pressures, which shows that the d_{50} decreases as the dispersion pressure increases. The span for each measurement on mannitol (□) and lysozyme (○) correspondingly increases, which reveals how measurement conditions can skew the traditional statistics used to characterize dry powders due to complicating factors, such as fragmentation.

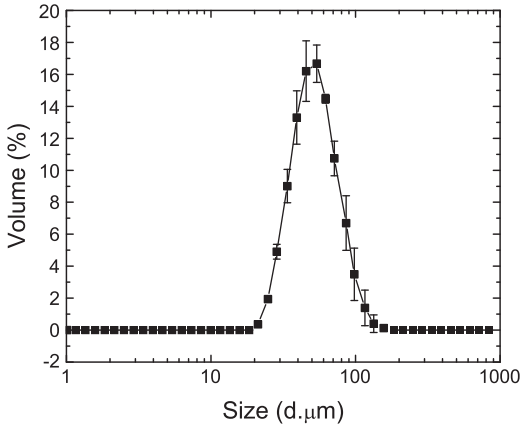

Fig. 3. Volume weighted particle size distribution of the deionized water droplets produced by the 40 kHz ultrasonic nozzle. The d_{mode} for the distribution is 48.3 μm.

3.3. Powder characterization

All BSA and lysozyme SFD powders were amorphous. For mannitol powders, high magnification SEM images revealed that the particles were highly porous and composed of aggregates of nanometer-sized, finger-like crystals of mannitol, as shown in Fig. 5a. The X-ray diffraction patterns for the SFD mannitol in Fig. 5b confirmed the sample crystallinity, and had many peaks corresponding to the raw mannitol which is the most thermodynamically stable polymorph, often referred to as the β form (Burger et al., 2000). However, there were several additional peaks, such as $2\theta = 9.7^\circ$ (Fig. 5b, inset), which have been shown to indicate the α polymorph of mannitol (Burger et al., 2000). The absence of a peak at $2\theta = 22^\circ$ makes it unlikely that the δ polymorph is present in the sample. In Fig. 5c, thermal analysis cannot confirm the presence of polymorphism in the sample due to the overlap of the melting curves for the α and β polymorphs at 166 °C (Burger et al., 2000). The apparent shoulder on the melting exotherm for the SFD mannitol, and lower enthalpy of transition compared to the single, symmetric peak for the raw material, further indicates the presence of polymorphism. The characteristic transition for the δ polymorph at 155 °C is not detected.

3.4. Powder dispersion

After powder dispersion in the NGI, recovery by dissolution and quantification of powder deposition on each stage using HPLC, the mass recovery was good for mannitol (102–114%) and lysozyme (94–119%) formulations. In contrast, there were significant interstage losses of BSA after dispersion, with only 62–73% of the dispersed mass recovered. The distribution of particle mass between the various stages of the NGI is graphed in Fig. 6. In the case

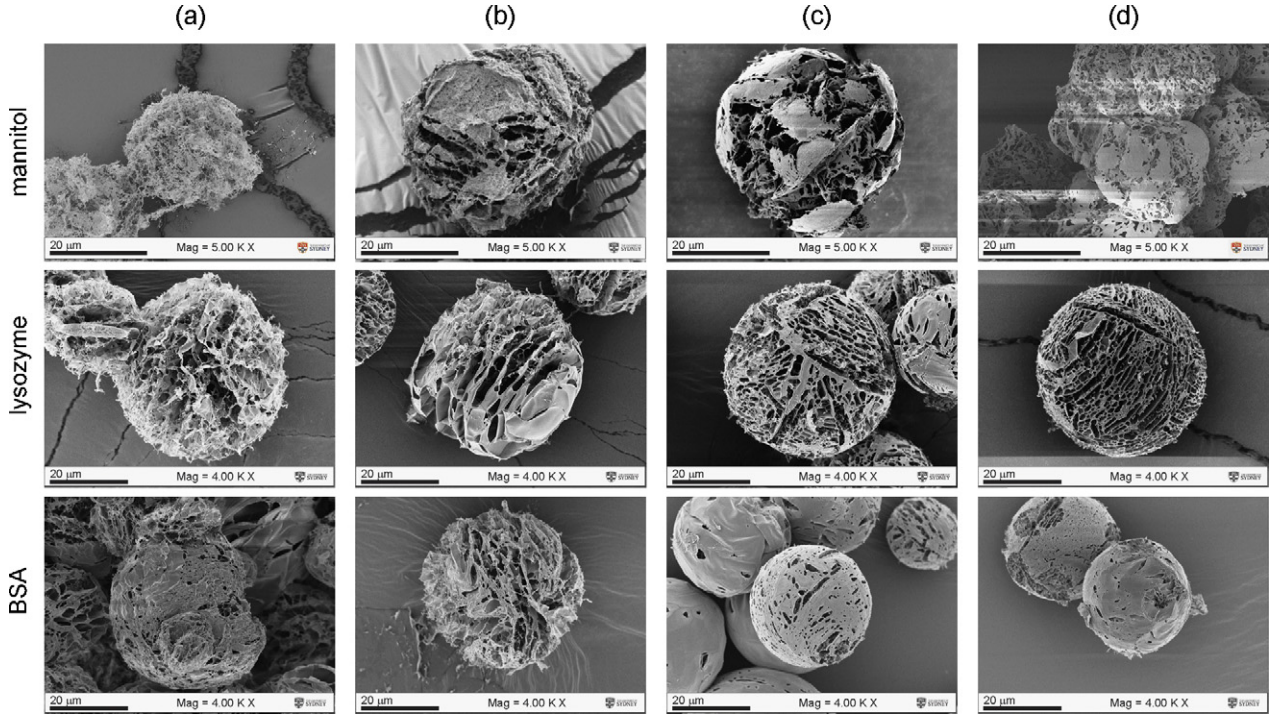

Fig. 4. SEM micrographs of representative mannitol, lysozyme and BSA particles prepared by SFD from aqueous solutions at (a) 1 wt%, (b) 2 wt%, (c) 4 wt%, or (d) 50 wt%, scale bar = 20 μm.

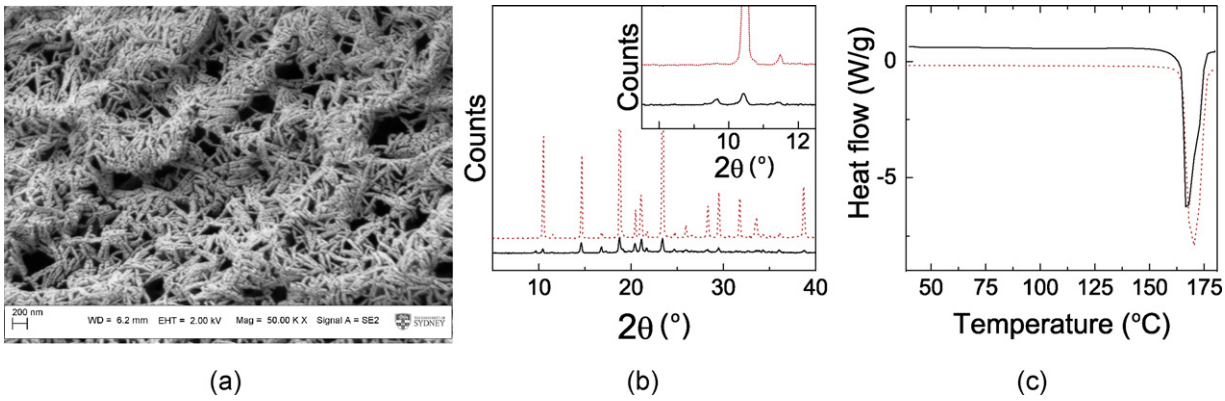

Fig. 5. Characterization of spray freeze dried powders of mannitol. (a) High magnification SEM image of the morphology of mannitol particles prepared from a 2 wt% solution from Fig. 3b; 50,000×, scale bar = 200 nm. (b) Powder XRD pattern for raw mannitol (. . .) and spray freeze dried mannitol (—). Inset magnifies low scattering angle intensity, highlighting the presence of new peaks in the spray freeze dried powder. (c) Data collected for a heat ramp on raw mannitol powder (. . .) and spray freeze dried mannitol (—), with one thermal transition corresponding to melting beginning at 166 °C.

of mannitol powders (Fig. 6a), the mass of particles impacting prior to S1 increased with c_s. Conversely, the mass of material recovered on S2 and beyond decreased with increasing c_s. These same two trends were observed for lysozyme particles (Fig. 6b). There were differing trends for dispersed BSA powders as c_s increased. There was a decrease in mass captured prior to S1 and an increase in material impacting on S1. There was no apparent trend on S2 and beyond, with consistently low levels of protein being recovered.

Particles recovered from S2 onwards were characterized by aerodynamic sizes (d_a) ≤6.1 μm. In order to determine the respirable fraction, or the Fine Particle Fraction (FPF), the fractions of mannitol with $d_a \leq 5$ μm by interpolation were summed together (2009) and plotted in Fig. 6 for each of the four formulations. For each formulation, the FPF was plotted against $c_s^{1/2}$. By an analysis of variance (ANOVA), there was no statistically significant dependence of the FPF on c_s ($P = 0.13$) for BSA formulations. However, there was such a dependence for mannitol and lysozyme particles, as determined by linear regression ($P < 0.05$).

4. Discussion

Considering that the rapid freezing of each atomized droplet in spray freeze drying results in the phase separation of solvent and solids in a confined volume, it follows that the solution composition should not affect the geometric dimensions of the particles formed, as found in Fig. 1. Neither the volume mean diameters nor the d_{50} values were used to compare the average particle size produced across formulations, as the presence of shoulders off the main peak skew these average values from the actual primary particle size produced, as well as increase the span. The features of the PSDs for each powdered formulation were attributed to properties of the dry powders and not the atomization step. We demonstrated this effect for mannitol and lysozyme in Fig. 2. The reported d_{50} for mannitol particles decreased dramatically initially, with little increase in span, as the dispersing pressure was increased from 0.5 to 1 bar which indicates that particle aggregates were being broken up. However, at a dispersion pressure of 3.5 bar, the span value increased dramatically and the d_{50} value approached a minimum. Furthermore, the fraction of particles less than 4 μm varied over multiple measurements of the same powder sample, which was attributed to particle fragmentation in the dispersing air stream. A similar series of measurements at various dispersion pressures on lysozyme particles resulted in a less pronounced decrease in size at very high dispersion pressures and a much smaller effect on the span, indicating that these particles are more robust and do not fragment like the mannitol particles. On the other hand, while BSA is not brittle, the substantial interstage losses of BSA during cascade impaction indicated that cohesion of BSA particles resulted in the presence of large aggregates which were difficult to disperse for laser light scattering measurements, and thus we obtained larger span values by laser diffraction. The small tail on BSA PSDs at the two higher concentrations may be due to satellite drops being produced for these most viscous samples, but the main peak location is very similar to the other concentrations. Since the lysozyme particles had mechanical integrity and low cohesive forces it was found to be the best material in terms of aerosolization.

The key parameter controlling the geometric size of particles was the ultrasonic nozzle frequency, which controlled the size of liquid droplets. Though not used while this work was being conducted, broadband ultrasonic generators capable of supplying variable frequency power are available, which can be used with interchangeable atomizing nozzles in order to tune the droplet size. The discrepancy between the measured d_{mode} for the dried particles and the deionzied water droplets may be due to a number of factors, but an important influence was contributed by the difficulty in assigning a suitable refractive index for the dried particles which were highly porous and multifaceted. The size analysis assumes a sphere with a uniform refractive index to deconvolute the scattering and determine the size and PSD. This assumption is true for aqueous water droplets but not the dried powders. We have looked at using an "average" refractive index, weighted by the volume fractions of air and mannitol. With this assumption, unphysically small particle diameters below 1 μm were reported. Therefore, we consistently used the refractive index for the pure material to analyze the scattering data and obtain values for d_{mode} which are reported in Table 1. A visual inspection of the resulting dry particles (Fig. 4) shows approximate aggreement with the sizes of the deionized water droplets produced by atomization (Fig. 3). The changing viscosity of the solution does not have a strong influence on droplet size since breakup is forced by the frequency or wavelength of the ultrasonic pressure field. For ultrasonic atomization at a constant 20 kHz frequency, Sears et al. (1978) demonstrated that a two order of magnitude increase in solution viscosity resulted in only a 20% change in median droplet size. Given that each of the four solutions of mannitol, lysozyme and BSA produced similar particle size distributions (Fig. 1), and that sizes by SEM of the dried particles were close to the measured aqueous liquid droplet sizes, we conclude that particles of approximately the same geometric size were

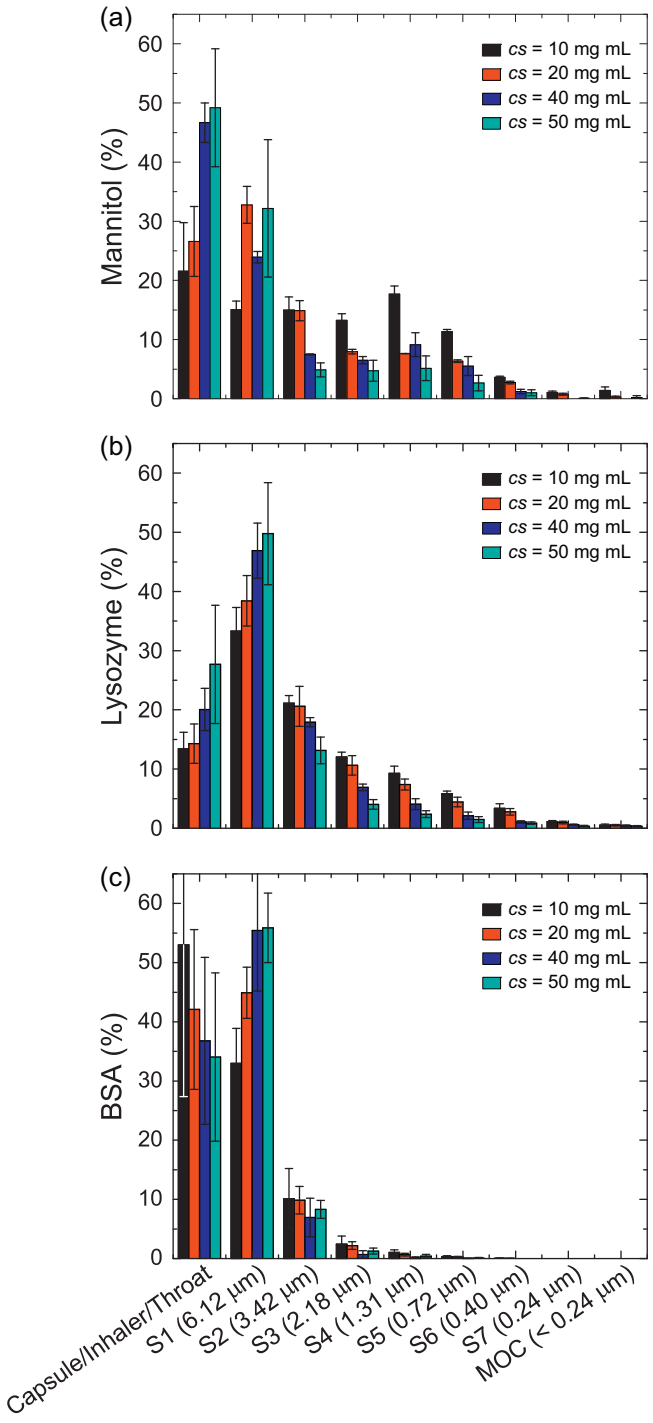

Fig. 6. Impaction data for each of the four SFD formulations of (a) mannitol, (b) lysozyme and (c) BSA, dispersed at 100 L min^{-1} in the Aerolizer®, where the fraction of the mannitol dose administered is plotted for each stage in the NGI. S1–S7 denote impactor stages 1–7, followed by the corresponding aerodynamic cutoff diameter in parentheses. MOC is the miro-orifice collector in the NGI. Error bars are SD for 3 replicates.

produced by spray freeze drying regardless of the c_s of the solute in the formulation. Despite having the same geometric size and similar porous morphology, the aerodynamic properties of each formulation varied significantly. Using an Aerolizer® dry powder inhaler (DPI), the powders were dispersed at 100 L min^{-1}, which corresponded to the inhalation flow a patient can achieve through the DPI using a comfortable inspiratory effort (Chew and Chan, 2001). For mannitol and lysozyme, the aerosol performance improved as c_s

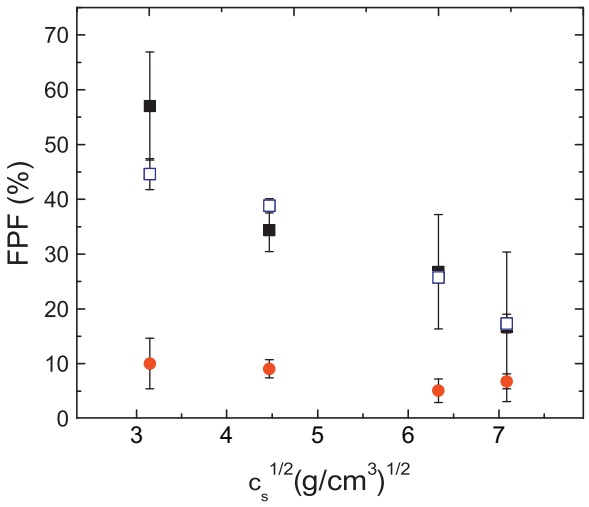

Fig. 7. The FPF for each formulation plotted as a function of the square root of the aqueous solution concentration. (■) Mannitol, (□) Lysozyme, and (●) BSA.

was decreased, i.e. as the porosity increased or the particle density decreased. Spray freeze drying produces powders with the same particle sizes, d_g, yet the amount of solute in each droplet varied with concentration in the liquid feed. Therefore, the particle density is proportional to the concentration of the starting solution. Previously, pure BSA particles produced from aqueous buffer at approximately 20 mg mL^{-1} yielded spray freeze dried powders with tap densities between 0.01 and 0.02 g cm^{-3} (Costantino et al., 2000). While this result is not a measure of the density of an individual particle due to the contributions of void spaces between particles, the close correlation between the mass concentration in the aqueous suspension and the tap density corroborates the expectation that the droplet volume does not change significantly during spray freeze drying and that ρ is determined by c_s. In this work, the SEM series for each set of powders in Fig. 4 shows the apparent density of material increasing with c_s. Therefore, given that d_g was constant, and that ρ was determined by c_s, d_a should be proportional to $c_s^{1/2}$. Indeed, we found in Fig. 7 for mannitol and lysozyme that the FPF, which was the fraction of particles with $d_a \leq 5$ μm, was linearly related to $c_s^{1/2}$. Furthermore, the FPF of mannitol and lysozyme formulations prepared at the same c_s have equivalent FPFs, despite the fact that one material was crystalline and the other amorphous. Thus, the FPF is determined only by c_s if the matrix material has good dispersibility. However, when the particles are cohesive, the aerosol performance is poor and independent of c_s.

5. Conclusions

In this work, we demonstrate the universality of using ultrasonic spray freeze drying to prepare large, porous particles from a range of water soluble materials. Rapid freezing produces particles of uniform sizes, the size is determined by the atomized feed droplet size, while the average particle density is determined independently by the solute concentration. Particles of different sizes could be produced using other ultrasonic frequencies for droplet atomization. The respirable fraction of powders produced in this way varies linearly with the square root of the particle density for mannitol and lysozyme, in agreement with the definition of the aerodynamic diameter, while the dispersion of BSA particles was poor, regardless of the particle density, due to significant particle–particle cohesion.

Acknowledgments

This work was supported through National Science Foundation and the Australian Academy of Science as part of the East Asia and South Pacific Summer Institutes Fellowship (Award number 1015344) and through grants from the Australian Research Council.

References

2009. Section 2.9.18 appendix XII C. Consistency of formulated preparations for inhalation. In: British Pharmacopoeia.

Amorij, J.P., Saluja, V., Petersen, A.H., Hinrichs, W.L.J., Huckriede, A., Frijlink, H.W., 2007. Pulmonary delivery of an inulin-stabilized influenza subunit vaccine prepared by spray-freeze drying induces systemic, mucosal humoral as well as cell-mediated immune responses in BALB/c mice. Vaccine 25, 8707–8717.

Bi, R., Shao, W., Wang, Q., Zhang, N., 2008. Spray-freeze-dried dry powder inhalation of insulin-loaded liposomes for enhanced pulmonary delivery. J. Drug Target. 16, 639–648.

Borgstrom, A., Clark, A., 2002. In vitro testing of pharmaceutical aerosols and predicting lung deposition from in vitro measurements. In: Bisgaard, H., O'Callaghan, C., Smaldone, G.C. (Eds.), Drug Delivery to the Lung. Marcel Dekker, Inc, New York, pp. 105–139.

Burger, A., Henck, J.O., Hetz, S., Rollinger, J.M., Weissnicht, A.A., Stottner, H., 2000. Energy/temperature diagram and compression behavior of the polymorphs of D-mannitol. J. Pharm. Sci. 89, 457–468.

Chew, N.Y.K., Chan, H.K., 2001. In vitro aerosol performance and dose uniformity between the Foradile® Aerolizer® and the Oxis® Turbuhaler®. J. Aerosol Med. 14, 495–501.

Costantino, H.R., Firouzabadian, L., Hogeland, K., Wu, C.C., Beganski, C., Carrasquillo, K.G., Cordova, M., Griebenow, K., Zale, S.E., Tracy, M.A., 2000. Protein spray-freeze drying. Effect of atomization conditions on particle size and stability. Pharm. Res. 17, 1374–1383.

D'Addio, S.M., Chan, J.G.Y., Kwok, P.C.L., Prud'homme, R.K., Chan, H.K., 2011. Constant size, variable density particles by spray freeze drying: aerosol delivery of antitubercular nanodrug-cocktails. In: AAPS Annual Meeting, Washington, DC.

Edwards, D.A., Hanes, J., Caponetti, G., Hrkach, J., BenJebria, A., Eskew, M.L., Mintzes, J., Deaver, D., Lotan, N., Langer, R., 1997. Large porous particles for pulmonary drug delivery. Science 276, 1868–1871.

Garmise, R.J., Staats, H.F., Hickey, A.J., 2007. Novel dry powder preparations of whole inactivated influenza virus for nasal vaccination. AAPS PharmSciTech 8.

Hinds, W.C., 1999. Aerosol Technology, Properties, Behaviors, and Measurement of Airborne Particles, 2nd ed. John Wiley & Sons, Inc., New York.

Lee, G., Sonner, C., Maa, Y.F., 2002. Spray-freeze-drying for protein powder preparation: particle characterization and a case study with trypsinogen stability. J. Pharm. Sci. 91, 2122–2139.

Maa, Y.F., Ameri, M., Shu, C., Payne, L.G., Chen, D.X., 2004. Influenza vaccine powder formulation development: spray-freeze-drying and stability evaluation. J. Pharm. Sci. 93, 1912–1923.

Maa, Y.F., Nguyen, P.A., Sweeney, T., Shire, S.J., Hsu, C.C., 1999. Protein inhalation powders: spray drying vs spray freeze drying. Pharm. Res. 16, 249–254.

Maa, Y.F., Shu, C., Ameri, M., Zuleger, C., Che, J., Osorio, J.E., Payne, L.G., Chen, D.X., 2003. Optimization of an alum-adsorbed vaccine powder formulation for epidermal powder immunization. Pharm. Res. 20, 969–977.

Mohri, K., Okuda, T., Mori, A., Danjo, K., Okamoto, H., 2010. Optimized pulmonary gene transfection in mice by spray-freeze dried powder inhalation. J. Control. Release 144, 221–226.

Nguyen, X.C., Herberger, J.D., Burke, P.A., 2004. Protein powders for encapsulation: a comparison of spray-freeze drying and spray drying of darbepoetin alfa. Pharm. Res. 21, 507–514.

Olschewski, H., Simonneau, G., Galie, N., Higenbottam, T., Naeije, R., Rubin, L.J., Nikkho, S., Speich, R., Hoeper, M.M., Behr, J., Winkler, J., Sitbon, O., Popov, W., Ghofrani, H.A., Manes, A., Kiely, D.G., Ewert, R., Siedentop, H., Seeger, W., 2002. Inhaled iloprost for severe pulmonary hypertension. New Engl. J. Med. 347, 322–329.

Qian, L., Zhang, H.F., 2011. Controlled freezing and freeze drying: a versatile route for porous and micro-/nano-structured materials. J. Chem. Technol. Biotechnol. 86, 172–184.

Saluja, V., Amorij, J.P., Kapteyn, J.C., de Boer, A.H., Frijlink, H.W., Hinrichs, W.L.J., 2010. A comparison between spray drying and spray freeze drying to produce an influenza subunit vaccine powder for inhalation. J. Control. Release 144, 127–133.

Sears, J., Huang, K., Ray, S., Fairbanks, H., 1978. Effect of liquid properties on production of aerosols with ultrasound. IEEE Trans. Son. Ultrason. 25, 131–133.

Sweeney, L.G., Wang, Z.L., Loebenberg, R., Wong, J.P., Lange, C.F., Finlay, W.H., 2005. Spray-freeze-dried liposomal ciprofloxacin powder for inhaled aerosol drug delivery. Int. J. Pharm. 305, 180–185.

Topp, M.N., Eisenklam, P., 1972. Industrial and medical uses of ultrasonic atomizers. Ultrasonics 10, 127–133.

Weers, J.G., Bell, J., Chan, H.K., Cipolla, D., Dunbar, C., Hickey, A.J., Smith, I.J., 2010. Pulmonary formulations: what remains to be done? J. Aerosol Med. Pulm. Drug Deliv. 23, S5–S23.

Zijlstra, G.S., Rijkeboer, M., van Drooge, D.J., Sutter, M., Jiskoot, W., van de Weert, M., Hinrichs, W.L.J., Frijlink, H.W., 2007. Characterization of a cyclosporine solid dispersion for inhalation. AAPS J. 9, E190–E199.